Chemical Engineering Journal 163 (2010) 256–263

Contents lists available at ScienceDirect

Chemical Engineering Journal

journal homepage: www.elsevier.com/locate/cej

Piecewise linear regression: A statistical method for the analysis of experimental adsorption data by the intraparticle-diffusion models

Gihan F. Malash, Mohammad I. El-Khaiary*

Chemical Engineering Department, Faculty of Engineering, Alexandria University, El-Hadara, Alexandria, Egypt

ARTICLE INFO

Article history:
Received 4 May 2010
Received in revised form 21 July 2010
Accepted 25 July 2010

Keywords:
Intraparticle-diffusion
Film diffusion
Adsorption
Piecewise linear regression
Mechanism

ABSTRACT

The film-diffusion and the intraparticle-diffusion models are widely used to analyze the mechanism of adsorption. The plots of these models often have a multi-linear nature, and in general, the graphical method is employed to analyze the data in which the linear segments are determined visually. This method suffers from subjectivity and therefore its estimated diffusion parameters are not very reliable. An alternative statistical method, piecewise linear regression (PLR) is presented and applied to experimental data. The results demonstrate that the use of PLR is practical and leads to diffusion estimates that may be quite different from the graphical method. PLR also determined the exact time periods for each diffusion regime, which opens new possibilities for analyzing and understanding the mechanism of diffusion. In order to encourage the testing and application of PLR, an easy to use Microsoft® Excel™ spreadsheet is made available.

1. Introduction

For practical applications of adsorption such as process design and control, it is important to model the adsorption rate and understand the dynamic behavior of the system. It is generally accepted that the adsorption dynamics consists of three consecutive steps [1]:

- Transport of adsorbate molecules from the bulk solution to the adsorbent external surface through the boundary layer diffusion.
- Diffusion of the adsorbate from the external surface into the pores of the adsorbent.
- Adsorption of the adsorbate on the active sites on the internal surface of the pores.

The last step, adsorption, is usually very rapid in comparison to the first two steps, and therefore, the overall rate of adsorption is controlled by the first or the second step, whichever is slower, or a combination of both. Many studies have shown that the boundary layer diffusion is the rate controlling step in systems characterized by dilute concentrations of adsorbate, poor mixing, and small particle size of adsorbent [2,3]. Whereas the intraparticle-diffusion controls the rate of adsorption in systems characterized by high concentrations of adsorbate, vigorous mixing, and large particle size of adsorbent. Also, it has been noticed in many systems that film diffusion (external mass transfer) is dominant at the beginning of adsorption during the initial adsorbate uptake, and then the adsorption rate becomes controlled by intraparticle-diffusion after the adsorbent's external surface becomes loaded with the adsorbate [1,2].

Many mechanistic models have been suggested to describe the adsorption kinetics. Two-resistance models, such as the film-solid model [4], the film-pore model [5], and the branched pore model [6], give detailed analysis of the adsorption dynamics. However, these models are presented as partial differential equations and their solution needs dedicated computer programs and extensive computer time. Therefore, it is impractical to use these models in industrial-plant simulations because in industry it is preferred to have more simple relations that can be solved quickly and easily. Even in the area of research, most researchers prefer to use simple lumped kinetic models to analyze their experimental results. At the present time, Boyd's [7] and Webber's [8] intraparticle-diffusion models are the two most widely used models for studying the mechanism of adsorption.

The film-diffusion model of Boyd is a single-resistance model that assumes that the main resistance to diffusion is in the boundary layer surrounding the adsorbent particle, this model is expressed as [7]:

$$F(t) = 1 - \left(\frac{6}{\pi^2}\right)\sum_{n=1}^{\infty}\left(\frac{1}{n^2}\right)\exp(-n^2Bt) \quad (1)$$

* Corresponding author. Tel.: +20 12 2175916; fax: +20 3 5921853.
E-mail addresses: El-Khaiary@Rocketmail.com, elkhaiary@gmail.com (M.I. El-Khaiary).

1385-8947/$ – see front matter © 2010 Elsevier B.V. All rights reserved.
doi:10.1016/j.cej.2010.07.059

Nomenclature

a_1 to a_n	the intercepts of the linear segments
A, B, C, D, ...	parameters of the general piecewise linear model
AIC	Akaike's Information Criterion
b_1 to b_n	slopes of the linear segments
Bt	a function of $F(t)$
D_i	the effective diffusion coefficient (cm^2/s)
DF	degrees of freedom
$F(t)$	the fractional attainment of equilibrium
J_1 to J_n	the breakpoints
k_i	intraparticle-diffusion parameter ($mg/g\,min^{0.5}$)
N	number of experimental data points
N_n	number of data points in the nth linear segment
N_p	number of parameters in the model
P	P value for hypothesis testing, it measures the probability of observing the sample data assuming the null hypothesis was true the in fact true
P_A	Akaike's weight, the probability that the model having the lower AIC is better than the alternative model
q	the dye uptake at time t (mg/g)
q_1	the dye uptake at the at the first breakpoint (mg/g)
q_e	the dye uptake at equilibrium (mg/g)
r	the radius of the adsorbent particle (cm)
R^2	coefficient of determination
S_X	the standard error of X
S_{YX}	the standard error of estimating Y
SSE	the sum of squared deviations
t	time (s)
t_1 to t_n	the time corresponding to the nth breakpoint
T_{conf}	the value of Student's t-distribution for a *confidence* % probability level,
X	the independent variable
Y	the dependent variable
Δ	the absolute value of the difference in AIC between the two models

where $F(t)$ is the fractional attainment of equilibrium, at different times, t, and Bt is a function of $F(t)$:

$$F(t) = \frac{q}{q_e} \tag{2}$$

where q and q_e are the dye uptake (mg/g) at time t and at equilibrium, respectively.

By applying the Fourier transform and then integration, Reichenberg [9] managed to obtain the following approximations:

$$\text{for } F(t) \text{ values} > 0.85, \quad Bt = 0.4977 - \ln(1 - F(t)) \tag{3a}$$

and

$$\text{for } F(t) \text{ values} < 0.85, \quad Bt = \left(\sqrt{\pi} - \sqrt{\pi - \left(\frac{\pi^2 F(t)}{3}\right)}\right)^2 \tag{3b}$$

B, can be used to calculate the effective diffusion coefficient, D_i (cm^2/s) from the equation:

$$B = \frac{\pi^2 D_i}{r^2} \tag{4}$$

where r is the radius of the adsorbent particle assuming spherical shape.

Eqs. (1)–(4) can be used in predicting the mechanistic steps involved in the adsorption process, i.e. whether the rate of removal of the dye takes place via particle diffusion or film-diffusion mechanism. This is done by plotting Bt against time, if the plot is linear and passes through the origin then intraparticle-diffusion controls the rate of mass transfer. If the plot is nonlinear or linear but does not pass through the origin, then it is concluded that film-diffusion or chemical reaction control the adsorption rate [7,9,10].

On the other hand, Webber's intraparticle-diffusion model is also a single-resistance model that was derived from Fick's second law of diffusion. This model assumes that:

(i) the external resistance to mass transfer (film diffusion) is not significant or only significant for a very short period at the beginning of diffusion;
(ii) the direction of diffusion is radial and the concentration does not change with angular position;
(iii) the intraparticle diffusivity is constant and does not change with neither time nor with position.

The intraparticle-diffusion parameter, k_i ($mg/g\,min^{0.5}$) is defined by the following equation:

$$q = k_i t^{0.5} \tag{5}$$

where q is the amount adsorbed (mg/g) at time t.

It can be seen from Eq. (5) that if intraparticle-diffusion is the rate limiting step, then a plot of q versus $t^{0.5}$ will give a straight line with a slope that equals k_i and an intercept equal to zero.

In spite of their apparent simplicity, the application of both the models of Boyd and Webber often suffer from uncertainties caused by the multi-linear nature of their plots. This multi-linearity is usually explained as follows: film-diffusion controls the rate of adsorption only in the initial time period, and therefore the plot of Bt versus t shows a curved line in the beginning of adsorption, eventually intraparticle-diffusion takes control of the overall adsorption rate, thus giving one or more new straight lines. It is up to the researcher to examine the plot and choose which points represent the first and second (and subsequent) segments. Similarly, the plot of q versus $t^{0.5}$ may show several linear segments, it has been proposed that the linear segments represent intraparticle-diffusion in pores of progressively smaller sizes [11], and again, it is up to the researcher to visually examine the plot and decide how many linear segments exist then choose the points to divide the plot into these linear segments.

The uncertainty in determining the linear segments leads to uncertainties in calculating their slopes and intercepts, and consequently, uncertainties in estimating the diffusion coefficients. Moreover, valuable results and conclusions are lost because a researcher can not accurately determine the time of transition from film to intraparticle-diffusion, and also the transitions between the consecutive intraparticle-diffusion regimes. If these transition times are accurately known, attempts can be done to correlate transition times to process variables such as agitation, particle size, pore size, concentration, q, etc.

The use of a statistical method to determine the beginning and end of each linear segment, and also the number of linear segments, would avoid the subjective decisions left to the researcher in the currently used graphical approach.

The objectives of this article are to present the method of piecewise linear regression as a tool for analyzing experimental adsorption dynamics results. Also, in order to facilitate the testing of this method, an easy to use Microsoft® Excel™ worksheet is made available that is capable of performing piecewise linear regression and applying statistical tests to the regression results. The results of this study would help researchers to get more accurate predictions of diffusion coefficients when applying the film-diffusion and the intraparticle-diffusion models to their experimental data.

2. Theory and calculations

2.1. Piecewise linear regression

Switching regression is a general class in statistical analysis whereby the independent variable, X, is segmented (divided into segments according to it's value) and the regression analysis is performed separately for these segments. The boundaries between the segments are called breakpoints. If it is required that the resulting regression equations does not show a discontinuity at the breakpoints, then this is a special case of switching regression, called piecewise regression.

Generally, the common equation of piecewise regression is expressed as [12]:

$$\begin{aligned} &Y = f_1(X), \quad X \le J_1 \\ &Y = f_2(X), \quad J_1 \ge X \ge J_2 \\ &\vdots \\ &Y = f_n(X), \quad X \ge J_n \end{aligned} \tag{6}$$

where Y is the dependent variable, X is the independent variable, and J_1 to J_n are the breakpoints.

In the special case where all segments are linear, the common equation becomes:

$$\begin{aligned} &Y = a_1 + b_1X, \quad X \le J_1 \\ &Y = a_2 + b_2X, \quad J_2 \ge X \ge J_1 \\ &\vdots \\ &Y = a_n + b_nX, \quad X \ge J_n \end{aligned} \tag{7}$$

where a_1 to a_n and b_1 to b_n are the intercepts and slopes of the linear segments, respectively.

Eq. (7) can be implemented in most nonlinear regression software. For example, in the case of one breakpoint, the common equation can be written as:

$$Y = A + BX + C(X - D)\ \mathrm{SIGN}(X - D) \tag{8}$$

and the values of A, B, C, and D are estimated by nonlinear regression. The Microsoft® Excel™ "SIGN" function determines the sign of a number then returns 1 if the number is positive, zero if the number is 0, and −1 if the number is negative.

The parameters of the common equation are then calculated as follows [13]:

$$J_1 = D, \qquad a_1 = A + CD, \qquad a_2 = A - CD, \qquad b_1 = B - C,$$
$$b_2 = B + C \tag{9}$$

The formula of Eq. (8) can be extended to any number of breakpoints:

$$Y = A + BX + C(X - D)\,\mathrm{SIGN}(X - D) + E(X - F)\,\mathrm{SIGN}(X - F) + \cdots \tag{10}$$

It can be seen from Eqs. (8) and (10) that the number of parameters, N_p, estimated by nonlinear regression is double the number of linear segments. Therefore, with a fixed number of experimental data points, N, the degrees of freedom of the common equation $(N - N_p)$ diminishes as the number of segments increase.

2.2. Nonlinear regression

Nonlinear regression estimates the model's parameters by the method of least squares. This is done by minimizing the sum of squared deviations, SSE, by numerical optimization techniques. The objective function for minimization is:

$$SSE = \sum_{i=1}^{N} (Y_{\mathrm{exp}} - Y_{\mathrm{est}})^2 \tag{11}$$

and the optimization routine searches for the set of parameter values that produce the smallest value of *SSE*. In order to do so, the spreadsheet presented here needs initial estimates of the parameters, and then it applies numerical optimization to minimize *SSE*. As a numerical procedure, the optimization routine keeps changing the parameter values until convergence is achieved. It should be noted that convergence may occur at a local minimum (not the global minimum), and therefore, it is necessary to repeat the nonlinear regression several times with different initial estimates of the parameters. From these repetitions, the global minimum is identified as the one having the smallest *SSE*. It was observed during testing the present spreadsheet that the initial estimates of the breakpoints have a strong effect on the final parameter estimates, while initial estimates of the other parameters had very little effect. In other words, poor initial estimates of the break points usually lead to convergence at local minima. Therefore, it is recommended to inspect the plot visually before regression to obtain reasonable initial estimates of the breakpoints.

2.3. Goodness of fit and parameter uncertainties

After finishing the nonlinear regression, the spreadsheet divides the data points into groups corresponding to the linear segments. For each linear segment, the coefficient of determination, R^2, is calculated by the built-in Excel™ function RSQ(Y values, X values). Also, the confidence limits for parameter estimates are calculated to asses their uncertainties. The confidence limits of the intercept of the nth line are calculated by [14]:

$$a_n \pm (T_{conf,N_n-2}) S_{YX} \sqrt{\frac{1}{\left(N_n - \sum X\right)^2 / \sum X^2}} \tag{12}$$

where a_n is the intercept of nth linear segment, T_{conf} is the value of Student's t-distribution for a *confidence %* probability level, N_n is the number of data points in the nth linear segment, S_X is the standard error of X, and S_{YX} is the standard error of estimating Y.

Similarly, the confidence limits of the slope of the nth line are calculated by [14]:

$$b_n \pm (T_{conf,N_n-2}) \frac{S_{YX}}{S_X \sqrt{N_n - 1}} \tag{13}$$

where b_n is the slope of nth linear segment.

2.4. Choosing the number of segments

Many statistical methods have been suggested to detect the number and locations of breakpoints. These methods include the use of Bayesian information criterion [15], likelihood-ratio test [16], and sequential comparison of confidence intervals [17]. Not only do these methods require extensive computations, but they also take the decision completely out of the hands of the researcher. This is sometimes a disadvantage due to the non-ideality of experimental adsorption results; the data points may be taken at uneven time intervals leaving blank periods, and also the experimental error in influential points may cause large bias in the estimates. Therefore, the method suggested here and demonstrated in the worksheet still allows the researcher to perform the conventional graphical analysis, but also ads statistical tools to help in reaching a decision about the number and location of breakpoints on a sound statistical basis.

The spreadsheet performs piecewise linear regression calculations for the cases of two, three, and four linear segments. It is suggested that the researcher examines the estimates of regression in the three cases, graphically assesses the segmented line produced, and check the confidence intervals of linear segments. If all estimates make sense and are also statistically accepted, then the next step is to compare models for the goodness of fit.

Increasing the number of linear segments increases the number of regression parameters, leading to a decrease in the degrees of freedom, and almost universally decreases *SSE*. Therefore, the goodness of fit cannot be based solely on *SSE* but must also include a penalty for the decrease in the degrees of freedom. Two well known statistical methods used in the comparison of models are based on the extra sum of squares method, these methods are the *F* test and Akaike's Information Criterion (*AIC*) [16]. The *F* test was derived from hypothesis testing and the analysis of variance (*ANOVA*). It should be emphasized that the *F* test is only valid for comparing nested models, it is fundamentally wrong to use it in comparing non-nested models. It involves analysis of the difference between the *SSE* of the two models being compared, taking into account the number of data points, N and the number of parameters, N_p, in each model. This information is used to calculate *F* ratio and *P* value as follows [17]:

$$F = \frac{(SSE_1 - SSE_2)/SSE_2}{(DF_1 - DF_2)/DF_2} \tag{14}$$

where SSE_1 and SSE_2 are the sum of squared deviations for the simpler and more complex model (the model that has more parameters), consecutively, while DF_1 and DF_2 are the degrees of freedom of the two models. After the *F* ratio is calculated, the *P* value is obtained from the *F* distribution using the Microsoft® Excel™ function FDIST (*F* ratio, DF_1, DF_2). The *P* value answers this question: If the simpler model was in fact correct, what is the probability of observing a random sample of data where the difference between SSE_1 and SSE_2 is as large (or larger) than obtained in this experiment? If the calculated *P* value is less than the chosen level of significance (usually 0.05) then it can be concluded that the complex model fits the data significantly better than the simpler model. Otherwise, the complex model is rejected because there is no statistical evidence that it fits the data better than the simpler model. It should be emphasized that the *F* test does not decide which model is correct; it just expresses the sufficiency of evidence for accepting/rejection of the simpler model.

AIC is based on information theory and maximum likelihood theory, and as such, it has an approach that is completely different from the *F* test and does not involve hypothesis testing. Rather, this method determines which model is more likely to be correct and quantifies how much more likely. For a small sample size, the corrected *AIC* is calculated for each model from the equation below [17]:

$$AIC = N \ln\left(\frac{SSE}{N}\right) + 2N_p + \frac{2N_p(N_p+1)}{N - N_p - 1} \tag{15}$$

The value of *AIC* can be positive or negative and its sign has no significance because it may change if the units expressing the data are changed, what really matters is the difference in *AIC* values between two models. The lower the *AIC* value (on a scale from $+\infty$ to $-\infty$) the better. The probability that the model having the lower *AIC* is better than the alternative model is calculated by [17]:

$$P_A = \frac{e^{0.5\Delta}}{1 + e^{0.5\Delta}} \tag{16}$$

where Δ is the absolute value of the difference in *AIC* between the two models. This probability is also called *Akaike's weight*. Another way of comparing *AIC* values is the *Evidence Ratio* which is defined by [17]:

$$Evidence \quad Ratio = \frac{1}{e^{-0.5\Delta}} \tag{17}$$

and it's numerical value means that the model with lower *AIC* is $1/e^{-0.5\Delta}$ times more likely to be correct than the alternative model.

2.5. Spreadsheet validation

As written, the spreadsheet can accommodate up to 40 data points. The nonlinear regression is performed using the Solver Add-In function to Microsoft® Excel™. By selecting the Options button in the Solver dialogue box, it is possible to modify the maximum number of iterations, maximum run time, percent tolerance, precision, and convergence criteria. The default settings were modified in the present spreadsheet as follows: number of iterations = 1×10^4, precision = 1×10^{-7}, tolerance = 5×10^{-4}% and convergence = 1×10^{-9}. Parameter constraints were also defined in the Solver dialogue box to make sure that the estimated breakpoints are all positive and are at progressively longer times. The spreadsheet produces best-fit parameter values, SSE, AIC, 95% confidence intervals of the parameters, Evidence Ratio, *P* values, and R^2 values for each linear segment.

All the calculations in this work have been performed by the spreadsheet and also by the commercial software package NCSS. The estimated values of the parameters obtained from the two software packages were always identical within $\pm 1 \times 10^{-2}$% difference, which can be attributed to minor differences in numerical calculations and rounding of numbers. This similarity in estimates shows that the more familiar and easily accessibly Excel™ spreadsheet is accurate enough to obtain reliable parameter estimates.

3. Application to experimental data

Due to their lack of a statistical method to handle multinearity, most researchers avoid the analysis of the multi-linearity in pore and film-diffusion plots. Some choose a few points and draw one straight line to calculate a pore-diffusion coefficient and ignore the remaining linear segments, while others fit a straight line to the entire adsorption period and naturally obtain poor fit to the data then conclude that pore diffusion does not control the rate of adsorption. Only a few published research articles acknowledge the presence of several segments and deal with these segments by the graphical analysis outlined above to study the variation of intraparticle-diffusion parameter as the adsorption progresses towards equilibrium. Among the authors who apply the graphical method to analyze multi-linearity in their articles are McKay [10], Allen [1,18], Kumar [19] and their co-workers. Their work is valuable because they have documented the temporal change of intraparticle-diffusion coefficient as adsorption takes place in smaller pores, and also presented studies that correlate the pore-diffusion coefficient with pore-size distribution and other adsorption variables. It is attempted in the present study to apply the statistical method, piecewise linear regression, to published experimental results of Koumanova et al. [1]. These experimental results show the effect of particle size on the adsorption of p-chlorophenol onto activated carbon. The following paragraphs present the detailed analysis of one adsorption data set (particle size 1000–1600 μm) to demonstrate the sequence of calculations and to present the recommended procedure. The final results for all particle sizes are presented to show the differences in estimates between the statistical and the graphical methods, and also to demonstrate how the statistical analysis provides deeper insight into the process and potentially provide more conclusions.

3.1. Applying PLR to Boyd's plot

3.1.1. General considerations

The statistical analysis is started by applying Boyd's model to the experimental results of the initial period of adsorption. The values of q at different times are entered in the *Data Input* worksheet, where $time^{0.5}$ values are automatically calculated. These values are

Table 1
Results of piecewise linear regression for the first two linear segments in the Boyd plots for different particle size of adsorbent. The values in parentheses are 95% confidence limits (D_i: cm^2/min; t_1: min).

Particle size	Slope 1	Intercept 1	t_1	Slope 2	Intercept 2
1000–1600 μm	0.00416 (0.00306–0.00525)	−0.0260 (−0.00420 to −0.0478)	<37.9	0.00841 (0.00504–0.0118)	−0.184 (−0.548 to 0.185)[a]
1600–2000 μm	0.00229 (0.00192–0.00266)	−0.0106 (−0.0182 to −0.00305)	<53.1	0.00590 (0.00480–0.00699)	−0.202 (−0.341 to 0.0631)
2000–2500 μm	0.00185 (0.00067–0.00302)	−0.0170 (−0.439 to 0.0194)	<51.5	0.00484 (0.00413–0.00555)	−0.171 (−0.656 to −0.277)

[a] The intercepts of the two linear segments at 1000–1600 μm are significantly different at 92% level.

copied automatically to the *Film Diffusion* worksheet where values of *Bt* are calculated from Eqs. (2) and (3) based on q_e value supplied by the user. It should be noted here that because *Bt* values are calculated from $\ln(1 - F(t))$, they become notoriously sensitive to changes in q when q_e is approached. For example, if a small experimental error in q (1%) changes the value of $F(t)$ from 0.95 to 0.9595, the value of *Bt* changes by 8.4% from 2.498 to 2.708. The same effect is even more exaggerated at higher values of $F(t)$. Therefore, it is not recommended to extend the Boyd plot to times close to equilibrium. This is done in the *Film Diffusion* worksheet by deleting the data corresponding to high *Bt* values. In the present study *Bt* values larger than 1.2 were not included in the calculations. It should be emphasized that the value of 1.2 is not a threshold or critical value, it is just a reasonable value chosen by the authors that include sufficient data to represent the first two segments. Also, in many kinetic studies the adsorption experiments are not extended long enough to reach equilibrium and therefore the value of q_e may not be known. It is possible in such cases to use an estimate of q_e obtained from fitting the data to pseudo kinetic models. It was found by many trials in the present study that the intercept of the first linear segment in the Boyd film-diffusion plot is not sensitive to changes in q_e, but the slopes and the breakpoint of the multi-linear Boyd plot change significantly with change of q_e. Therefore, if the value of q_e is not known with certainty then the Boyd plot can only be used to estimate the intercept (which tells if this time period is controlled by film diffusion or not) but cannot be used to obtain accurate estimates of both the slope (needed to calculate the diffusion coefficient) and the time corresponding to the breakpoint. Another decision is in order here regarding whether to include the point ($time = 0$, $q = 0$) or not. It is recommended to exclude this point because at the very beginning of adsorption what really takes place is the liquid filling the pores and wetting the outer and inner surfaces, this is neither film nor pore diffusion, and therefore, if this point is included it will result in a biased estimate of the intercept and consequently may result in a wrong conclusion about the mechanism taking place.

3.1.2. PLR results

By applying this treatment to the experimental data of Koumanova et al. [1] for particle size 1000–1600 μm it was found that the intercept of the first linear segment in the Boyd plot is −0.0260 with 95% confidence limits of (−0.0042 to −0.0478). This value of the intercept is significantly different from zero, and this strongly suggests that film diffusion is the rate controlling mechanism during the first 38.2 min of adsorption. This is further corroborated by the low R^2 value of this segment (0.965) and also by the obvious nonlinearity of the points in the first segment in the plot. It should be remembered that the time value at the breakpoint is not reliable because of the absence of an accurate value of q_e for this system. The results of applying SLR to Boyd plots of all particle sizes of the adsorbent are presented in Table 1 and the plots of the first two linear segments are shown in Fig. 1.

3.2. Applying PLR to Weber's plot

The next step is to apply Weber's pore-diffusion model to the same set of experimental data. The sequence of calculations is illustrated in the flow sheet in Fig. 2. The values of q at different times are automatically copied to worksheets that perform piecewise linear regression based on the assumption of 2, 3, and 4 linear segments, these worksheets are named L-L, L-L-L, and L-L-L-L, consecutively. The user then switches to these worksheets, enters initial estimates for the regression parameters, and consequently reaches the best fit for each case. A decision about the number of linear segments is reached by means of the *Evidence Ratio* and *F ratio* calculated by the worksheets. For the particle size 1000–1600 μm, the *AIC* values for L-L and L-L-L are −12.8 and −26.4. This large difference means that three linear segments is much more likely to be the correct model than two linear segments, and the evidence ratio of 883 means that L-L-L is 883 times more likely to be the correct model than L-L. The same conclusion is also reached from the *P value* that is calculated from the *F ratio*, the value of $P = 3.4 \times 10^{-5}$ is much smaller than the usually accepted 0.05 significance level. In other words, there is only a 0.0034% probability of observing the current *F* ratio if the L-L model is in fact correct. Therefore, it is concluded that three linear segments is statistically a better fit than 2 linear segments.

By applying a similar comparison between three and four linear segments, it was found that *AIC* values for L-L-L and L-L-L-L are −26.4 and −23.5 which suggests that L-L-L is more likely to be the correct model, but the corresponding *evidence ratio* of 4.13 means that L-L-L is only 4.13 times more likely, which is not considered overwhelming evidence in favor of L-L-L model [17]. The *P value* is 0.024 which is smaller than the accepted 0.05 significance level, and indicates that the complex model (L-L-L-L) fits the data significantly better than the simpler model (L-L-L). Therefore, it is decided to accept the model with four linear segments as the correct model. The shape of the data points' trend does not suggest more

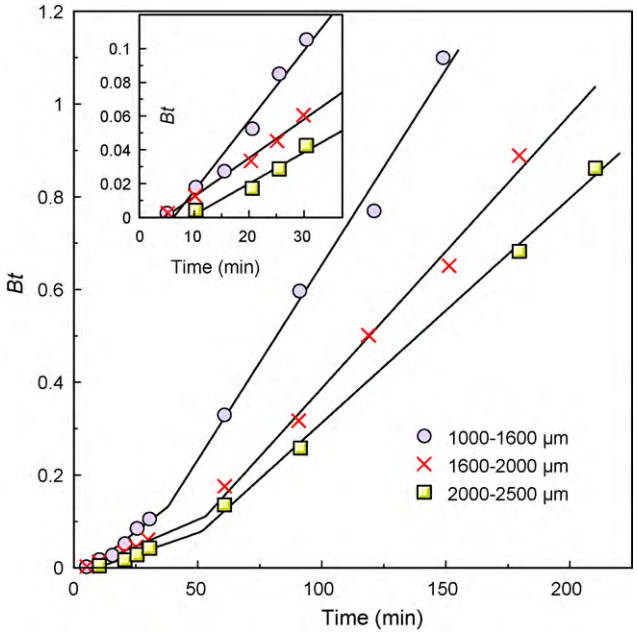

Fig. 1. Boyd plots for the initial period of adsorption of p-chlorophenol onto activated carbon of different particle sizes.

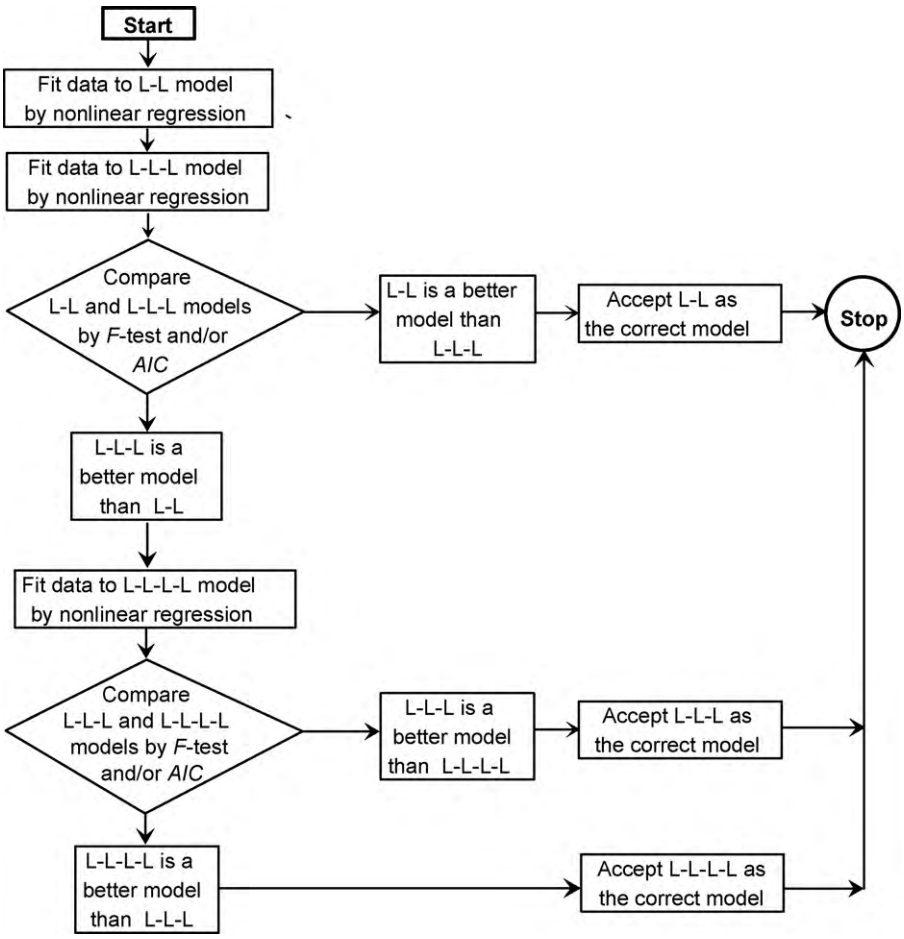

Fig. 2. Flow sheet illustrating the steps of calculations to choose the number of linear segments in the model.

than four segments, accordingly, more complex models were not tested.

By observing the results of fitting four linear segments to the pore-diffusion model for the experimental results of particle size 1000–1600 μm shown in Table 2, it is seen that the intercept of the first linear segment is −3.561 with 95% confidence limits of (−4.220 to −2.903) which is significantly different from zero, and since the same linear segment has an intercept of −0.0260 in the Boyd plot, it is concluded that the rate in this initial period of adsorption is controlled by film diffusion. The time corresponding to the end of the first linear segment, and consequently to the end of film diffusion, is estimated from L-L-L-L to be 82.3 min which is quite different from the value of 37.9 min estimated from the regression of Boyd's plot. However, the break point estimated from Boyd's plot is not reliable in our specific case as discussed above, and therefore, a value of 82.3 min is accepted for the breakpoint and will be used in the discussion that follows.

Fig. 3 and Table 2 show the intraparticle-diffusion plots for different adsorbent particle sizes. It is seen that the adsorption begins with a period of fast film diffusion, followed by slower periods of intraparticle diffusion as the system approaches equilibrium. One major difference between the plots in Fig. 3 and the same plots obtained by graphical analysis done by Koumanova et al. is that according to the statistical analysis there is strong evidence for the presence of four linear segments in case of particle size 1000–1600 μm, while the graphical analysis produced only three segments. It is also noticed that the statistical analysis only yields three linear segments for particle sizes 1600–2000 and 2000–2500 μm. This may possibly be explained as follows: the inside surface area of a porous medium is the sum of the pore surfaces of three different kinds of pores that exist in the material. The through pores extend from one end to the other, the blind pores end inside the material, and the closed pores are not accessible [20]. As the particle size decreases, more closed pores are transformed to blind pores and become accessible for adsorption, thus changing the size distribution of accessible pores. Another possible explanation is that the presence of gaps (regions without experi-

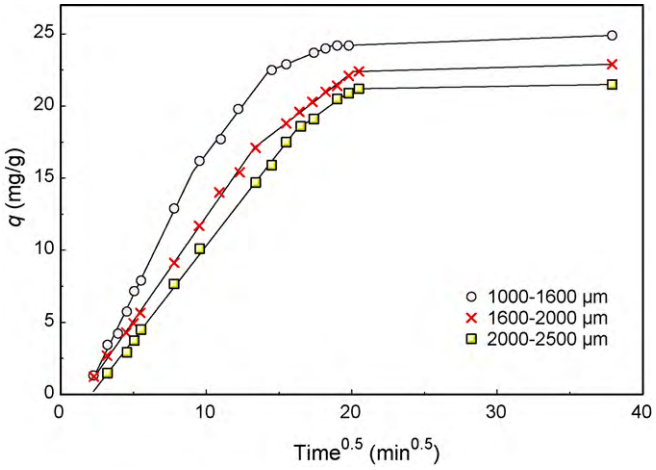

Fig. 3. Intraparticle-diffusion plots adsorption of p-chlorophenol onto activated carbon of different particle sizes.

Table 2
Comparison between the intraparticle-diffusion results of the present study and the results of Koumanova et al. (k_i: mg/g min$^{0.5}$; t_i: min).

Particle size	k_1	t_1	k_2	t_2	k_3	t_3	k_4	t_4
1000–1600 μm								
Koumanova et al.	1.8911	<136.9	0.9539	136.9–265.7	0.0435	>265.7	–	
This study	2.0935 (1.922–2.265)	<82.3	1.3418 (−1.275 to 3.96)	82.3–203.6	0.4088 (0.387–0.430)	203.6–345.5	0.0378 (0.0198–0.0558)	>345.5
1600–2000 μm								
Koumanova et al.	1.4366	<179.6	0.7895	179.6–392.0	0.0385	>392.0	–	–
This study	1.4399 (1.400–1.479)	<184.1	0.7492 (0.679–0.819)	184.1–407.2	0.0287 NP	>407.2	–	–
2000–2500 μm								
Koumanova et al.	1.3022	<269.0	0.6978	269.0–388.1	0.0339	>388.1	–	–
This study	1.3026 (1.262–1.343)	<259.8	0.7310 (0.518–0.944)	259.8–404.4	0.0172 NP	>404.4	–	–

NP: it was not possible to calculate confidence limits because the line consists of two data points.

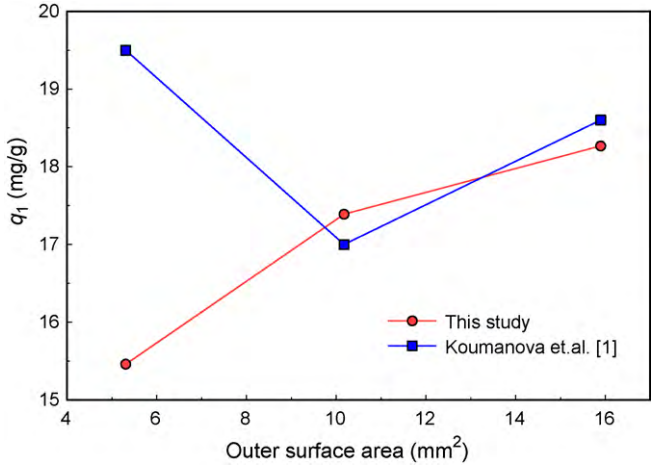

Fig. 4. The variation of q_1, the p-chlorophenol uptake on the outside surface of carbon, with the outside surface area of carbon (assuming spherical shape).

mental data) in the cases of 1500–2000 and 2000–2500 μm sizes is responsible for missing a breakpoint that occurs in one of these gaps. Experimental evidence is needed to back the correct explanation. This evidence would be the pore-size distribution for each size fraction and also more kinetic data points.

Table 2 also presents k_i values for different intraparticle-diffusion regimes and also t_i, the breakpoints or the times of transition between diffusion regimes. It is observed that some of the values obtained in the present study are similar to those obtained by the graphical analysis done by Koumanova et al. [1], while other values are very different. Although these differences may seem unimportant, it will be shown in the following discussion that they have a significant impact on the conclusions about the mechanism taking place in this adsorption system.

To our best knowledge, adsorption research until now does not pay attention to the times of transition between consecutive diffusion regimes, nor to the significance of q_1, the dye uptake at the time of transition from film to intraparticle-diffusion control. Fig. 4 shows the relationship between q_1, the dye uptake supposed to take place by film diffusion, and the outer surface area of the adsorbent (assuming spherical shape). It is seen in the figure that the values of q_1 estimated by the graphical method has no apparent trend, while q_1 estimated in the present study has an almost linear relationship with the outside surface area and this corroborates the assumption that the amount q_1 is adsorbed on the outer surface.

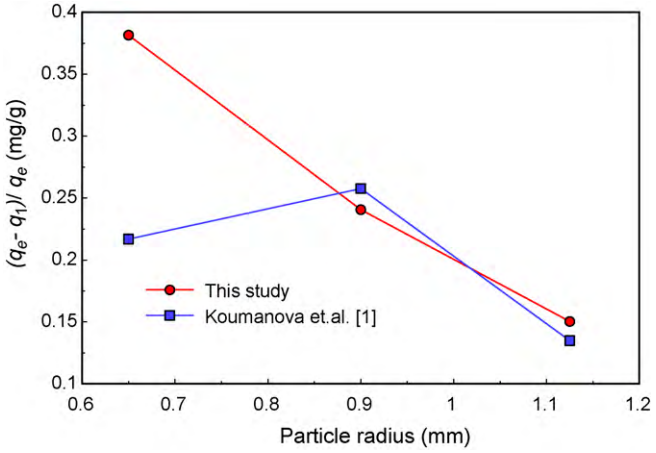

Fig. 5. The variation of the fraction of p-chlorophenol uptake inside the pores of carbon with the particle radius.

Another way of utilizing q_1 values is shown in Fig. 5, where the fraction adsorbed in the pores $(q_e - q_1)/q_e$ is plotted against the particle radius. A linear relation is obtained that is in agreement with the known phenomena of increasing available pore surface with the decrease in particle size. This kind of analysis, presented in Figs. 4 and 5, reveals interesting relations between breakpoints and variables of the adsorption system. The present study does not suggest any new theories, it only highlights new possibilities for analyzing adsorption data. If similar analysis is routinely carried out by researchers, the results may possibly lead to better insight into the mechanism of adsorption.

4. Conclusions

The reduction of subjectivity in scientific research is necessary, no matter what discipline. The method of PLR has been presented as a complement to the traditional graphical method for the analysis of multi-linear intraparticle-diffusion plots. It has been demonstrated in the present work that the calculations are practically straightforward, and thanks to the abundance of computers and software, little training is needed to master this method.

The breakpoints are assumed to represent transition between diffusion regimes. Until now, they were not utilized in interpreting experimental results, probably due to the ambiguity in determining their values by the graphical method. The present study shows that the breakpoint values estimated by PLR, being obtained by sound statistical methods, open new prospects in the interpretation of kinetic adsorption data.

The reliability of the PLR analysis can be enhanced by the experimental design of the kinetic study. First, it would be beneficial to have as many kinetic data points as possible, this would ensure having a reasonable number of points in each segment and thus obtaining statistically significant estimates of the diffusion parameters. And secondly, a data set with no gaps (blank regions with no observations) would help in determining the location of breakpoints with more accuracy.

Appendix A. Supplementary data

Supplementary data associated with this article can be found, in the online version, at doi:10.1016/j.cej.2010.07.059.

References

[1] B. Koumanova, P. Peeva, S. Allen, Variation of intraparticle diffusion parameter during adsorption of p-chlorophenol onto activated carbon made from apricot stones, J. Chem. Technol. Biotechnol. 78 (2003) 582–587.
[2] M.S. Ray, Adsorption and adsorptive separations: a review and bibliographical update, Adsorption 2 (1996) 157–178.
[3] D. Mohan, K.P. Singh, Single and multicomponent adsorption of cadmium and zinc using activated carbon derived from bagasse—an agricultural waste, Water Res. 36 (2004) 2304–2318.
[4] X. Yang, S.R. Otto, B. Al-Duri, Concentration-dependent surface diffusivity model [CDSDM]: numerical development and application, Chem. Eng. J. 94 (2003) 199–209.
[5] R.G. Lee, T.W. Weber, Non-isothermal adsorption in fixed beds, Can. J. Chem. Eng. 47 (1969) 54.
[6] X. Yang, B. Al-Duri, Application of branched pore diffusion model in the adsorption of reactive dyes on activated carbon, Chem. Eng. J. 83 (2001) 15–23.
[7] G.E. Boyd, A.W. Adamson, L.S. Myers Jr., The exchange adsorption of ions from aqueous solutions by organic zeolites, II: Kinetics, J. Am. Chem. Soc. 69 (1947) 2836–2848.
[8] W.J. Weber, J.C. Morris, Kinetics of adsorption on carbon from solution, J. Sanitary Eng. Div. Proc. Am. Soc. Civil Eng. 89 (1963) 31–59.
[9] D. Reichenberg, Properties of ion exchange resins in relation to their structure. III. Kinetics of exchange, J. Am. Chem. Soc. 75 (1953) 589–598.
[10] S.H. Jeong, K. Park, Drug loading and release properties of ion-exchange resin complexes as a drug delivery matrix, Int. J. Pharm. 361 (2008) 26–32.
[11] Y.S. Ho, G. McKay, The kinetics of sorption of basic dyes from aqueous solution by Sphagnum moss peat, Can. J. Chem. Eng. 76 (1998) 822–827.
[12] G.A.F. Seber, C.J. Wild, Nonlinear Regression, John Wiley & Sons, New York, 1989.
[13] J.L. Hintze, NCSS User's Guide, NCSS, Kaysville, USA, 2006.
[14] J. Ermer, J.H.McB. Miller, Method Validation in Pharmaceutical Analysis: A Guide to Best Practice, John Wiley & Sons Inc., New York, 2005.
[15] D.W.K. Andrews, Tests for parameter instability and structural change with unknown change point, Econometrica 61 (1993) 821–856.
[16] J. Bai, Likelihood ratio tests for multiple structural changes, J. Econom. 91 (1999) 299–323.
[17] H. Motulsky, A. Christopoulos, Fitting Models to Biological Data Using Linear and Nonlinear Regression, Oxford University Press, Oxford, 2004.
[18] S.J. Allen, Q. Gan, R. Matthews, P.A. Johnson, Mass transfer processes in the adsorption of basic dyes by peanut hulls, Ind. Eng. Chem. Res. 44 (2005) 1942–1949.
[19] A. Kumar, S.H. Kumar, S. Kumar, Adsorption of resorcinol and catechol on granular activated carbon: equilibrium and kinetics, Carbon 41 (2003) 3015–3025.
[20] P. Klobes, K. Meyer, R.G. Munro, Porosity and Specific Surface Area Measurements for Solid Materials. National Institute of Standards and Technology, Spec. Publ. 960-17, Washington, DC, 2006.